

Phase oscillations in superfluid $^3\text{He}-\text{B}$ weak links

 A. Smerzi^{1,a}, S. Raghavan^{2,3,b}, S. Fantoni^{1,2}, and S.R. Shenoy²
¹ Istituto Nazionale di Fisica della Materia and International School for Advanced Studies, 34014, Trieste, Italy

² Abdus Salam International Center for Theoretical Physics, 34100, Trieste, Italy

³ Rochester Theory Center for Optical Science & Engineering, Department of Physics & Astronomy, University of Rochester, Rochester NY 14627, USA

Received 19 March 2001

Abstract. Oscillations in quantum phase about a mean value of π , observed across micropores connecting two $^3\text{He}-\text{B}$ baths, are explained in a Ginzburg-Landau phenomenology. The dynamics arises from the Josephson phase relation, the interbath continuity equation, and helium boundary conditions. The pores are shown to act as Josephson tunnel junctions, and the dynamic variables are the inter bath phase difference and fractional difference in superfluid density at micropores. The system maps onto a non-rigid, momentum-shortened pendulum, with inverted-orientation oscillations about a vertical tilt angle $\phi = \pi$, and other modes are predicted.

PACS. 03.75.Fi Phase coherent atomic ensembles; quantum condensation phenomena – 67.57.-z Superfluid phase of liquid ^3He – 74.50.+r Proximity effects, weak links, tunneling phenomena, and Josephson effects

The search for Josephson-like weak-link effects in superfluids has a long history [1–7]. In order to see Josephson-like phenomena, the characteristic length-scale of the weak-link should be comparable to the temperature-dependent coherence length $\xi(T)$. Thus a candidate superfluid is $^3\text{He}-\text{B}$, with a relatively large zero-temperature coherence length $\xi(0) \sim 65$ nm [8]. In fact the oscillatory displacement of flexible membranes walling off $^3\text{He}-\text{B}$ baths connected by micropores, induces a Josephson-like, periodic current-phase relation [3–7]. Recently, Davis, Packard, and collaborators have observed a remarkable phenomenon: metastable oscillations of $^3\text{He}-\text{B}$ with an average phase-difference of π across the weak link [6]. The explanation of these, and other complex tunneling oscillations is of considerable general interest, since they provide examples of novel macroscopic quantum effects.

Bose-Einstein condensate (BEC) tunneling of neutral atoms between double-well traps has been predicted [9] to support π -state oscillations, and other modes. The coupling between the $N_{1,2}$ condensate atoms in wells 1, 2, with phase difference ϕ is $-\sqrt{N_1 N_2} \cos \phi \sim -(1 - z^2)^{1/2} \cos \phi$ where $z = (N_1 - N_2)/(N_1 + N_2)$ is the fractional population imbalance. The coupling energy corresponds to [10] a *non-rigid* pendulum [9, 11] of tilt angle ϕ , momentum $p_\phi = z$ and length $(1 - p_\phi^2)^{1/2}$. The non-rigid pendulum is shortest when moving fastest, and can thus support inverted-orientation oscillations about $\phi = \pi$ (concave downwards).

The BEC mapping onto a non-rigid pendulum dynamics is the generic consequence of wave function phase factors and the two-state nature of the tunneling: properties that it shares with the $^3\text{He}-\text{B}$ system. However, the BEC dynamics cannot be naively taken over [12]: features of the constrained helium wavefunction in a pore geometry, must play a role.

In this paper we show that the helium wave function boundary conditions in a pore geometry, in conjunction with the Josephson phase relation and the continuity equation, determine the $^3\text{He}-\text{B}$ tunneling dynamics, that is indeed similar to non-rigid pendulum dynamics, but with a (momentum-dependent) torsion-bar [13] due to hydrodynamic flows outside the pore [4]. Thus *dynamical* π -states of temperature-dependent frequency can occur, with a rich variety of other modes.

The wavefunction is depressed by the boundary conditions (bc) inside, and just outside a pore length, that is shown to act as a tunneling barrier, for sufficiently narrow pores. Displacements of the flexible membrane wall are proportional to a fractional shift z of the depressed wavefunction, that acts as an oscillating “Josephson piston”: it conveys pairs through the tunneling region at a rate ($\sim \dot{z}$) determined by the (sine of) the phase difference ϕ_J across the pore. We now derive the (quasiequilibrium) $^3\text{He}-\text{B}$ dynamics.

Free Energy: The $^3\text{He}-\text{B}$ order parameter [8] can be written as $\Phi_{\mu,i}(\mathbf{r}) = \Psi(\mathbf{r})B_{\mu,i}(\mathbf{n}(\mathbf{r}))$, where $\Psi(\mathbf{r}) = |\Psi(\mathbf{r})|e^{i\phi(\mathbf{r})}$ and $|\Psi(\mathbf{r})|$ is proportional to the gap, varying on a coherence length $\xi(T)$. Here $\mathbf{B}(\mathbf{n}(\mathbf{r}))$ is a tensorial factor, with “ $\mathbf{n}(\mathbf{r})$ ” representing axis rotations, varying over a textural healing length $l_{\text{tex}}, \geq 5 \mu\text{m}$ [8].

^a e-mail: smerzi@sissa.it

^b Present address: Corning Incorporated, Corning, NY 14831, USA

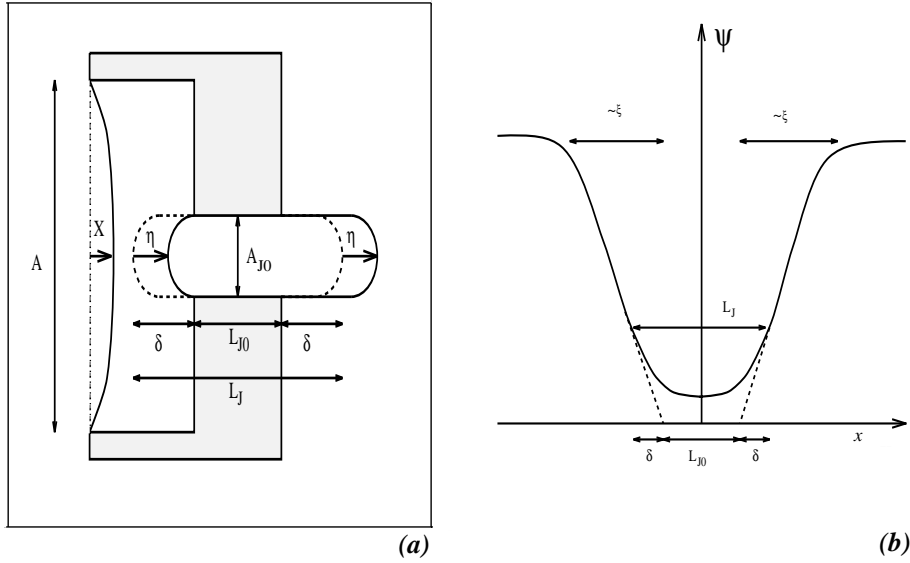


Fig. 1. Schematic diagrams (not to scale) of: (a) Effective pore/bath geometry, showing geometric pore length L_{J0} and pore (bath) area A_{J0} (A). Dashed line shows the rest position of the “Josephson piston” of length $L_J = L_{J0} + 2\delta$. The piston shift is η and the membrane displacement is $X(\propto \eta)$. (b) Equilibrium wavefunction $\psi(x)$ versus x .

The Ginzburg-Landau (GL) free energy is a scalar, with traces over the tensorial products: $F(\{\Phi(\mathbf{r}), \nabla\Phi(\mathbf{r})\}) = F_0(\{\Phi(\mathbf{r})\}) + F_{\text{grad}}(\{\nabla\Phi(\mathbf{r})\})$ [8]. Unlike the superconductor bc of vanishing normal gradients of the gap, we must use here “helium” bc, with the order parameter vanishing at the walls, $\Phi_{\mu,i}(\mathbf{r}) \rightarrow 0$. This bc, supported by experiment, has been used elsewhere [14], and is particularly relevant in the system regime [5–7] of pore scales $\sim \xi$, $\ll l_{\text{tex}}$. The bc is enforced by $\Psi \rightarrow 0$ over length scales $\sim \xi$, and the contributions to F_{grad} from $|\nabla\Psi|$ contributions will dominate those from $|\nabla B| \sim |\nabla n|$ [15]. The $\mathbf{n}(\mathbf{r})$ textural variables can be set equal to their fixed, bath value, [8]. Thus $F_{\text{grad}} \rightarrow F_{\text{grad}}(\{\nabla\Psi(\mathbf{r})\})$, and the effective free energy describing the pore region is

$$F = \int d^3r \left[\frac{\hbar^2}{2m^*} |\nabla\Psi(\mathbf{r})|^2 + a\epsilon|\Psi|^2 + \frac{b}{2}|\Psi|^4 \right] \quad (1)$$

where a, b, m^* are GL coefficients (constants in space and time) absorbing tensorial-factor traces of order unity; and $\epsilon = (T/T_c - 1)$, where T_c is the transition temperature.

The experimental geometry [5] is a superfluid of total mass density ρ in a pillbox of cross-section A , and length L , closed at one end by a flexible membrane (of spring constant C) and at the other end by a perforated wall with $N_J = 65 \times 65$ pores of geometric cross-section A_{J0} and length L_{J0} . The pillbox bath is immersed in a larger superfluid bath. (See Fig. 1). We consider a single pore. The x coordinate is along the pore axis, and the system cross-section $A(x)$ varies between A and A_{J0} .

To obtain an effectively 1D model, we average over the transverse cross-section of the system, and scale in the equilibrium wave function $|\Psi_0| = (a|\epsilon|/b)^{1/2}$ where the effective superfluid mass density is $\rho_s(T) = m^*|\Psi_0|^2 \sim |\epsilon|$. Thus the 1D gap wavefunction is $\psi(x) = [\Psi(\mathbf{r})]/|\Psi_0|$, where $[\dots] \equiv \int d^2r(\dots)/A(x)$. With $\xi(T)^2 = \hbar^2/(2m^*a|\epsilon|)$, the

free energy from equation (1) is:

$$F \simeq \epsilon_0 \int dx A(x) \left[\xi^2 |\partial_x \psi|^2 + (U - 1)|\psi|^2 + \frac{1}{2}|\psi|^4 \right] \quad (2)$$

where the energy density is $\epsilon_0 \equiv |\Psi_0|^2 a |\epsilon| \sim |\epsilon|^2$. The averaged transverse gradients $U(x) = [|\partial_y \Psi(\mathbf{r})|^2 + |\partial_z \Psi(\mathbf{r})|^2]/|\Psi(\mathbf{r})|^2$ are $\sim \xi^2/A_{J0}$ in the pore region, and negligible, $\sim \xi^2/A$ in the bulk. Thus $U(x)$ is an effective energy barrier, arising from the bc. We set $U(x) = \gamma^2 \xi^2/A_{J0}$ in an effective barrier length $|x| < L_J/2$, and zero outside it. The barrier length L_J is greater than the geometric pore length L_{J0} , as the wave function depression (and large transverse gradients) will persist by continuity, for a small distance or “overhang”, outside the pore openings, of size $\delta = (L_J - L_{J0})/2$ as shown in Figure 1. We treat $\gamma, > 1$, as a fitting parameter, and consider $e^{-KL_J} \ll 1$ as small.

Wavefunctions: The barrier region solutions of the (linearized) GL equation derived from equation (2) are $e^{\pm Kx}$, with a real decay wavevector $K \equiv \sqrt{(\gamma^2/A_{J0}) - \xi^{-2}}$, for $\sqrt{A_{J0}} < \gamma\xi$. (An estimate, for square pores, is $\gamma = \sqrt{2\pi}$.) With a phase difference $\phi_J \equiv \phi(x = L_J/2) - \phi(x = -L_J/2)$ across the junction, the (dimensionless) pore wavefunctions are in a form [4] generalized to

$$\psi(x) = [a_- e^{-i\phi_J/2} \sinh K((L_J/2) - x) + a_+ e^{i\phi_J/2} \sinh K((L_J/2) + x)] / \sinh KL_J, \quad (3)$$

where coefficients a_{\pm} here match on to bath wave functions, rather than plane waves [4]. Substitution into equation (2) yields a leading-order, $|x| \leq L_J/2$ contribution

$$F_J = -E_J \sqrt{(a_+^2 a_-^2)/a_0^4} \cos \phi_J, \quad (4)$$

neglecting $O(e^{-2KL_J} \cos 2\phi_J)$ corrections. The Josephson energy is $E_J \equiv 2A_{J0}K\xi^2\epsilon_0 a_0^2 f(T)/\sinh KL_J$, and $f(T)$ is a possible renormalization factor discussed later. We now estimate a_{\pm} amplitudes and their dependence on interbath pair transfers.

Equilibrium wave-functions deep in the baths 1, 2 are rigid, as bulk $^3\text{He-B}$ is incompressible. Solutions of the nonlinear GL equation from equation (1) are hyperbolic tangents, flat in the bulk and falling to zero with slope $1/\sqrt{2}\xi$ at walls [1]. We take the averaged bath wavefunction as $\psi_{1,2}(x) = e^{\mp i\phi_J/2} g(\mp x - L_{J0}/2)$, where $g(x) = \tanh(x/\sqrt{2}\xi)$. At $x = \mp L_J/2$, continuity with equation (3) yields equal equilibrium pore-amplitudes $a_- = a_+ \equiv a_0$, and $a_0 = g_0$, where the bath wavefunction at the barrier edge is $g_0 \equiv g(\delta)$. See Figure 1. Slope-matching determines the (weakly T -dependent) overhang δ as $\sinh(\sqrt{2}\delta/\xi) = \sqrt{2}/K\xi \coth((K(L_{J0} + 2\delta)/2))$. For long narrow pores, $g_0 \sim \delta/\sqrt{2}\xi$, and the overhang $\delta \simeq 1/K \sim A_{J0}^{1/2}$ vanishes, as pores close, $A_{J0} \rightarrow 0$.

Slowly oscillating and small ($X(t) \ll \xi$) displacements of the far-off flexible membrane will be transmitted by the rigid bulk, to induce shifts by $\eta(\propto X)$ of the wavefunction near the pores. Since η will be related to the tunneling through the pores, we term the movable region of length L_J in Figure 1, a ‘‘Josephson piston’’. The bulk wavefunctions at $x = \mp L_J/2 + \eta$ then match onto the (shifted) piston equation (3), yielding a_{\pm} . For small η , defining $z \equiv 2\eta/\delta$ as a fractional piston-overhang shift, we can expand as $\sqrt{a_+^2 a_-^2/a_0^2} \sim \sqrt{1-z^2}$ to obtain equation (4) as $F_J = F_J(\phi, z)$. (Additional wavefunction stiffness terms, $F_J \sim +z^2$ make $z = 0$ the piston rest position; these are dominated by membrane stiffness terms, given later).

The shift of the interfaces between the Josephson region and the bath to $x = -\frac{1}{2}L_J + \eta$, $x = \frac{1}{2}L_J + \eta$ means that there are increases/decreases in the number of atoms in the two tunneling overhang regions. Note that z can be interpreted as a fractional imbalance [9] of the overhang volumes $2A_{J0}\delta$, and is *not* a fraction of the total Cooper pairs [12].

Clearly, the incremental number change $dn_{1,2}$ in each bath will be the number density at the interface times the incremental shift $d\eta$. The change in tunneling population $dn = \frac{1}{2}(dn_1 - dn_2)$ from the overhangs on the two sides is then [16] $dn = -(\rho A_{J0} g_0^2 \delta / 2m_3) dz$ where m_3 is the helium atom mass. The piston displacements induce a reactive velocity component [16] of the membrane $\dot{X} \propto \frac{1}{2}(g_0^2 \delta) \dot{z}$ proportional to the tunneling current.

Current Equation: The tunneling current (piston velocity) equation for \dot{z} is provided by the continuity equation $\dot{\rho}(r) = \nabla \cdot \mathbf{J}(r)$ where \mathbf{J} is the total mass current density. Integrating over baths 1, 2 (outside the piston regions) and using Gauss's theorem, $m_3 \dot{n} = \frac{1}{2} A_{J0} ([J_x(x = -L_J/2)] + [J_x(x = L_J/2)])$. Assuming no normal fluid flows through the narrow pores, and with superfluid mass-current density $[J_x(x)] = \rho_s \frac{\hbar}{m^*} \text{Im}(\psi^* \partial \psi / \partial x)$, equa-

tion (3) yields:

$$\frac{\hbar}{2K_J} \frac{dz}{dt} = -\sqrt{1-z^2} \sin \phi_J = -\frac{\partial H}{\partial \phi_J}. \quad (5)$$

where H and K_J are defined below. The physical picture is of phases at N_J pore openings in each bath locked together, and with a common difference between baths, so that the 4000 Josephson pistons vibrate in unison.

Phase Equation: The Josephson relation for $\phi = \phi_2 - \phi_1$, the total interbath phase difference, is $\dot{\phi} = \Delta\mu/\hbar$ and the chemical potential difference from the tunneling transfer of n atoms will contribute as $\Delta\mu \simeq -\partial F_J/\partial n$. (The bulk contributions from the incompressible, constant-density fluid in the baths, clearly cancel out of the difference $\Delta\mu$.) Work done by a fixed [7] external pressure P_{ext} , and by the Josephson piston, pushing against the membrane, of spring constant C , can also be included [16]. Thus

$$\frac{\hbar}{2K_J} \frac{d\phi}{dt} = \Lambda z + \frac{P_{\text{ext}}}{P_J} + \frac{z}{\sqrt{1-z^2}} \cos \phi_J = \frac{\partial H}{\partial z}; \quad (6a)$$

$$H = \frac{1}{2} \Lambda z^2 + \frac{P_{\text{ext}} z}{P_J} - \sqrt{1-z^2} \cos \phi_J, \quad (6b)$$

where $P_J \equiv \rho K_J/m_3$ is a pressure scale. The frequency scale is $2K_J/\hbar \equiv (\rho_s/\rho)(2\hbar K/m^* \delta) f(T)/\sinh(KL_J) \sim |\epsilon| f(T)$; and $\Lambda \equiv (Cg_0^2 \delta)/(2AP_J) \sim C/f(T)$ is a (dimensionless) membrane stiffness parameter.

Note that ϕ and z are not canonically conjugate, as $\phi \neq \phi_J$ due to hydrodynamic effects [4]. The hydrodynamic bath-pore superflow $I = (A_h/A_{J0}) A_{J0} \rho_s (\hbar/m^*) (\phi_h/L_h)$ is driven by a phase gradient ϕ_h/L_h over a hydrodynamic length L_h in each bath. (Here A_h/A_{J0} is a bath-pore ‘‘transmission probability’’). The same current $I = I_J \sqrt{1-z^2} \sin \phi_J$, tunnels through the pore, where the Josephson critical (mass) current is $I_J = E_J 2m_3/\hbar \sim |\epsilon|^2 f(T)$. With total phase change $\phi = 2\phi_h + \phi_J$, we have a nonlinear relation [4] generalized to $\phi = \phi(\phi_J, z)$:

$$\phi = \phi_J + \alpha \sqrt{1-z^2} \sin \phi_J, \quad (7)$$

where $\alpha \equiv (2\frac{A_{J0}}{A_h})(KL_h g_0^2 f(T))/\sinh(KL_J) \sim |\epsilon| f(T)$. This corresponds to a torsion-bar as in the inductive SJJ case [10, 13], but now, momentum-dependent.

The temperature-dependence of $\Lambda(T)$ is essentially that of $f(T)$. Experimentally, the critical current goes as $\sim (1 - T/T_{\text{ca}})^2$, appearing to vanish before transition, at a $T_{\text{ca}} = 0.91T_c$ [6]. Since $I_J \sim \epsilon^2 f(T)$, this ‘‘experimental’’ form $f(T) = (1 - T/T_{\text{ca}})^2/\epsilon^2$, could be used. Or, $f(T)$ could be attributed to thermal phase fluctuations [17]. We estimate it, in this picture [18].

Equations (5–7) constitute the model equations for the $^3\text{He-B}$ system, in terms of the mutually linked dynamics of the fractional Josephson piston shift $\eta/\delta \equiv z/2$ and the phase difference ϕ_J across it. They can be solved in terms of elliptic functions [16] just as in the $\alpha = 0$ ‘‘BEC-like’’ case [9]. They correspond to a non-rigid pendulum of tilt

angle ϕ_J , and angular momentum z , with a momentum-dependent torsion bar. The torsion-bar [13] induces hysteretic effects for $\alpha \geq 1$. We focus on $\alpha < 1$ where the modes are essentially as for $\alpha = 0$, with the equations predicting five distinct undriven modes (instead of the two of the rigid pendulum). The modes can be visualized by plotting [11] the locus of the pendulum coordinates ($\sqrt{1-z^2} \sin \phi_J, -\sqrt{1-z^2} \cos \phi_J$). With a dc drive P_{ext} there is an ac Josephson oscillation at a frequency $\omega_{\text{ac}} = 2m_3 P_{\text{ext}} / \rho \hbar$; with added resonant ac drives, there are Shapiro-like dc current spikes [9,16]. “Zero-state” oscillations of the pendulum can occur, with time averaged $\langle \phi \rangle = 0 = \langle z \rangle$. The pendulum, once excited, can rotate freely, with a running phase, and a “self-trapped” piston-shift/membrane-displacement $\sim \langle z \rangle \neq 0$.

Since the non-rigid pendulum is shortest, when moving fastest, it can execute small “inverted” oscillations about an average value of $\langle \phi \rangle = \pi$. These $\Lambda \lesssim 1$, “ π -state oscillations”, with $\langle z \rangle = 0$, and are *dynamically* metastable, with the momentum-shortened pendulum “digging a well for itself” by its motion. Finally, there are two types of $\Lambda > 1$, “ π -state rotations” with self-trapped $\langle z \rangle \neq 0$ and $\langle \phi \rangle = \pi$, (on either side of a fixed point $\phi = \pi, z = \sqrt{1-\Lambda^{-2}}$). These correspond to the non-rigid pendulum executing closed-loop trajectories, floating above the point of support [9,11]. Damping of π -state oscillations through the non-rigid pendulum velocity $\dot{\phi}$, or the momentum z , behave quite differently. While the former [11] drives the system to rest at $\phi_J = 0$, the latter [16] damps it to $\phi_J = \pi$.

We use values [6] $L_{J0} = 0.5 \times 10^{-5}$ cm, $A_{J0} = 10^{-10}$ cm², $\rho = 0.08$ g/cm³, $m^* \simeq 2m_3 = 10^{-23}$ g, $N_J = 4225$, $\xi(0) = 65$ nm, $A = 0.7$ cm², $C = 10^6$ dynes/cm, $T_c = 0.91$ mK, and a purely illustrative parameter $\gamma \simeq 23$. Then $\delta \simeq 90$ Å and $2K_J(0)/\hbar \simeq 400$ Hz, $(I_J(0)/m_3) \simeq 3.2 \times 10^6$ atoms/sec, corresponding to a Josephson energy per pore $E_J(0) \simeq 0.02 k_B T_c$. We find $\Lambda(0) \simeq 0.9$; $P_J \simeq 0.35$ mPa; and $\alpha(0) \simeq 0.5$.

The results of our model are shown in Figure 2. The dimensionless membrane displacement *versus* dimensionless time ($t2K_J/\hbar \rightarrow t$) is shown for zero- and π -states. The insets show the temperature-dependent frequencies and critical currents. These include: i) zero-state oscillations, with harmonic frequencies $\omega_0(T) = [(1+\Lambda)/(1+\alpha)]^{1/2} (2K_J/\hbar)$ that vary from kHz, to zero at T_c . ii) π -state oscillations, with smaller amplitudes and frequencies $\omega_\pi(T) = [(1-\Lambda)/(1-\alpha)]^{1/2} (2K_J/\hbar) < \omega_0(T)$, that vanish on warming, when $\Lambda(T)$ crosses unity, well before T_c . iii) A critical current [19] ($\lesssim 20$ picogram/s) goes as ϵ^2 , appearing to vanish before T_c . iv) With a phase angle defined as the time-integrated membrane displacement [6], the current-phase relations (not shown) have same-sign, positive slopes in the zero- and π -states.

Our model (with a single chosen parameter γ that estimates the rapid wavefunction variation inside the pore), reproduces many observed features and magnitudes. In experiments, oscillations about an average $\langle \phi \rangle = 0$ exist below T_c and have a typical angular frequency scale of hundreds of hertz, while oscillations about $\langle \phi \rangle = \pi$ appear only on cooling well below T_c and are lower in

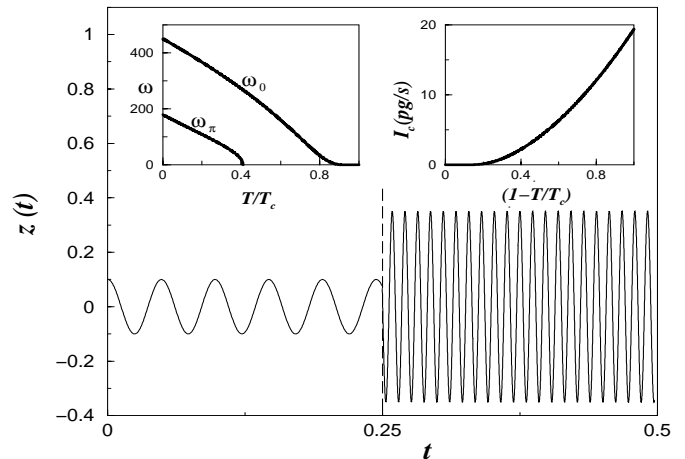


Fig. 2. Dimensionless $z(t)$ (proportional to membrane displacement) *versus* dimensionless time for $|\epsilon| = 1$, and parameters as in text. π -state oscillations (early times); are kicked out to zero phase oscillations (later times). Left inset: Zero-state (π -state) angular frequencies $\omega_0(T)$ ($\omega_\pi(T)$) defined in text, *versus* temperature. Right inset: Characteristic current $\mathcal{I}_c \propto I_J(T)$ the Josephson critical current, as defined in text, *versus* temperature.

frequency [6]. The scale for the pressure-drive in the ac Josephson effect is millipascals [5]. The maximum mass-transport current per pore $I_c(T)$ is of order ten picograms/sec and vanishes well before T_c [5,6]. These values and behaviours can be compared with Figure 2 and the numerical estimates of the text. Our model also predicts self-trapped π -states with $\omega_\pi^{\text{tr}} = [(A^2 - 1)/(1 - \alpha/\Lambda)]^{1/2} (2K_J/\hbar)$, that have not yet been reported.

Further work could include experimental investigations of predicted intermode transitions with frequencies dipping to zero, as $\Lambda(T)$ or $z(0), \phi(0)$ are varied through critical values [9,16]; and a search for self-trapped π -states.

π states have been related to a static metastable minimum induced by spin-textures in the baths [20]. This could dress our dynamic π states from oscillations of the density depression at pores, producing fine structure in the oscillation modes. In fact, bistability between two types of π oscillations has been reported [21]. The first discussion about π -states and half-flux quantization, in connection with d-wave Cooper pairing, was given in the context of high T_c superconductors in [22].

In conclusion, we have modelled the dynamics of $^3\text{He-B}$ baths closed by flexible walls, and connected by micropores. The dynamic equations arise from helium boundary conditions, the continuity equation, and the Josephson phase relation. The dynamical variables are the phase difference, and the shift of the pore wave-function overhang, beyond the geometric pore length. The system maps on to a non-rigid momentum-shortened pendulum dynamics. The π -phase oscillations observed in $^3\text{He-B}$ have features similar to those predicted by the model. Other tunneling modes are predicted.

It is a pleasure to thank J.C. Davies, R.E. Packard, E. Granato, M. Mehta, R. Simmonds and S. Vitale for useful conversations. We thank R.E. Packard for providing unpublished data. This work was partly supported by the Cofinanziamento MURST and by the NSF Grant PHY94-15583.

References

1. D. Tilley, J. Tilley, *Superfluidity and Superconductivity* (Adam Hilger, Bristol and New York, 1990).
2. P.W. Anderson, *Rev. Mod. Phys.* **38**, 298 (1966).
3. O. Avenel, E. Varoquaux, *Phys. Rev. Lett.* **55**, 2704 (1985); *Phys. Rev. Lett.* **60**, 416, (1988).
4. E. Varoquaux, O. Avenel, G. Ihas, R. Salmelin, *Physica B* **178**, 309 (1990).
5. S. V. Pereverzev, A. Loshak, S. Backhaus, J.C. Davis, R.E. Packard, *Nature* **388**, 449 (1997).
6. S. Backhaus, *et al.* *Nature* **392**, 687 (1998); *Science* **278**, 1435 (1998)
7. R.W. Simmonds, *et al.* *Phys. Rev. Lett.* **81**, 1247 (1998).
8. D. Vollhardt, P. Wolfe, Chap. 7, *The Superfluid Phases of Helium-3* (Taylor and Francis, London, 1990).
9. a) A. Smerzi, S. Fantoni, S. Giovannazzi, S.R. Shenoy, *Phys. Rev. Lett.* **79**, 4950 (1997); b) S. Raghavan, A. Smerzi, S. Fantoni, S.R. Shenoy, *Phys. Rev. A* **59**, 620 (1999).
10. The superconductor Josephson junction (SJJ), by contrast, corresponds to a *rigid* pendulum with (charged) Cooper pair imbalances suppressed by the external circuit/Coulombic energy costs, as noted in [9].
11. I. Marino *et al.*, *Phys. Rev. A* **60**, 1 (1999).
12. A direct carryover of our BEC dynamics (as done *e.g.* by N. Hatekenaka, *J. Phys. Soc. Jpn* **67**, 3672 (1998)) is clearly unphysical: with $N_{1,2} \sim 10^{23}$ Cooper pairs, and $N_1 - N_2 \leq 10^{14}$ pairs transferred in a cycle, the fractional Cooper pair imbalance $z \leq 10^{-9}$ is quite negligible. z must correspond to some other fraction.
13. T.A. Fulton, in *Superconductor Applications*, edited by B. Schwarz, S. Foner (Plenum, 1976).
14. S. Ullah, A.L. Fetter, *Phys. Rev. B* **39**, 4186 (1989).
15. Textural variation work focusses on the opposite regime of scales $\sim l_{\text{tex}}$, with the gap set equal to a constant.
16. S. Raghavan, A. Smerzi, S. Fantoni, S.R. Shenoy, unpublished.
17. E. Granato, private communication.
18. A Gaussian “spin-wave” average of phase factors with a coupling energy proportional to $N_J E_J \sim |\epsilon|^2$ yields an estimate of $f(T) \sim e^{-(T/T_c)(\epsilon_1/\epsilon)^2}$, and typically, $\epsilon_1 \sim 0.2$. The singular flattening of this $f(T)$ at $T = T_c$ makes it seem to vanish at a “ T_{ca} ” $< T_c$. The stiffness $\Lambda(T) = \Lambda(0)/f(T)$ diverges at T_c .
19. If the measured signal in the \dot{X} membrane velocity is presented as a mass current $\mathcal{I} \equiv \rho A \dot{X}/N_J$ [6], then a related characteristic current is $\mathcal{I}_c = (A/N_J A_J) I_J$.
20. S.K. Yip, *Phys. Rev. Lett.* **83**, 3864 (1999); J.K. Vilj, E.V. Thuneberg, *Phys. Rev. Lett.* **83**, 3868 (1999) and [cond-mat/0107052](#). These models work in the “pin-hole” regime of $\sqrt{A_{J0}}/\xi, L_{J0}/\xi \rightarrow 0$ with a fixed-ratio $L_{J0}/\sqrt{A_{J0}} < 1$. In this pinhole limit, our “Josephson piston overhang” vanishes, $\delta/\xi \rightarrow 0$: our pore-size regime is, instead, nonzero $\sqrt{A_{J0}}/\xi \sim L_{J0}/\xi \sim 1$.
21. A. Marchenko *et al.*, *Phys. Rev. Lett.* **83**, 3860 (1999).
22. V.B. Geshkenbein, A.I. Larkin, A. Barone, *Phys. Rev. B* **36**, 235 (1987).